*Int. J. Electrochem. Sci.*, 11 **(2016)** 7453 – 7460, doi: 10.20964/2016.09.45

International Journal of
ELECTROCHEMICAL
SCIENCE
www.electrochemsci.org

# Facile PVP-Assisted Synthesis of $MnO_2$@MWNT Composites and their Application in Supercapacitors

*Yong Qian, Chenling Huang, Rong Chen, Shizhen Dai, Chunyan Wang*[*]

Jiangxi Key Laboratory for Mass Spectrometry and Instrumentation, East China University of Technology, Nanchang 344000, P.R. China
[*]E-mail: chywang9902@163.com

*Received:* 16 June 2016 / *Accepted:* 19 July 2016 / *Published:* 7 August 2016

A composite of well dispersed $MnO_2$ nanoparticles adhered on multi-walled carbon nanotubes ($MnO_2$@MWNT) is obtained through facile hydrothermal process and followed by high temperature annealing. The nanoscale $MnO_2$ particles were homogeneously distributed on the surface of MWNTs under polyvinyl pyrrolidone (PVP)-assisted reaction. The $MnO_2$@MWNT composite (34.43 wt. % $MnO_2$) displays a high specific capacitance of 285.12 F/g at a current density of 1 A/g in 1 M $Na_2SO_4$ electrolyte. The electrode exhibits good cycling stability, which the specific capacitance retention retains up to 90.17% after 1000 cycles at 1 A/g.

**Keywords:** Supercapacitor; $MnO_2$@MWNT; PVP-assisted synthesis

## 1. INTRODUCTION

Recently, the rapid growing market demand for low cost, safe and environmentally friendly energy sources has irritated plentiful research achievement in the progressive electrode materials for energy storage/conversion devices [1]. Supercapacitors (SCs) have attracted considerable attention as high power density, faster charging/discharging rate, excellent cycling stability and wide working temperature range, which make SCs extremely competitive among multifarious types of electrochemical energy storage devices [2, 3]. SCs can be split into electrical double-layer capacitors (EDLCs) and pseudocapacitors depending on their energy storage mechanism. EDLC usually use carbon or carbon material modified electrodes and store energy via the separation of charge in the electrical double-layer at the interface between the electrode and electrolyte. Pseudocapacitors usually employ metal oxides and conducting polymers modified electrodes and achieve Faradaic storage through the redox reaction between the electrode material and the electrolyte [2,4].

Manganese oxide ($MnO_2$), as a kind of high-performance electrode material received great interests because of its low cost, high theoretic capacitance (about 1370 F/g), excellent cycle stability

and environmental friend [5, 6]. However, the electrical conductivity $MnO_2$ is poor, and the structure is densely packed lead to smaller surface area. These characteristics limit its application in the development of excellent supercapacitors. To overcome these difficulties, an ideal structure has been put forward combined $MnO_2$ nanostructures with conductive carbon materials. It can increase the charge-discharge rate and cycling performance through improve the electrical conductivity greatly and obtain better capacitance performance with higher specific capacitance, power density and energy density[6].

One dimensional (1D) carbon materials, including single-walled carbon nanotubes (SWNTs) and multi-walled carbon nanotubes (MWNTs), are relatively new materials that have recently received extensive attention because of their excellent chemical, physical, mechanical, optical and electrical properties [7-9]. Carbon nanotubes (CNTs) have been considered as attractive electrode materials for high-performance SCs. due to their good electrical conductivity, chemical and mechanical stability, and high surface area [10-13]. CNTs can not only be used as an electrode material of electrical double-layer capacitors, but also act as a support to form hybrids with other electrode materials to improve electrochemical performances [14, 15].

Herein, we prepared $MnO_2$@MWNT composites through PVP-assisted hydrothermal process and high temperature annealing. The nanoscale $MnO_2$ was homogeneously distributed on the MWNTs, which have been confirmed by TEM, XRD and XPS analysis. The composite (31.26 wt.% $MnO_2$) exhibits a high specific capacitance of 285.12 F/g at a 1 A/g in 1 M $Na_2SO_4$ electrolyte and good cycling stability.

## 2. EXPERIMENTAL

### *2.1. Synthesis of $MnO_2$@MWNT composites*

MWNTs with the lengths of 0.1-10 μm were purchased from Nanjing XFNano Technology Co., Ltd. (China), and were purified according to literature [16] prior to use. The other chemicals were bought from Aladdin reagent Co., Ltd. (China) and used without further purification. The solutions were prepared with ultrapure water (>18MΩ).

A 100mg purified MWNTs and 50mg PVP were mixed and dispersed fully into 200 mL deionized water in three-neck flask under stirring at 50°C for 6 hr, then 40 mg $MnSO_4{\cdot}H_2O$ was added to the flask. After another 1hr of stirring, 2mL of 30% $H_2O_2$ were stepwise added into the mixture, and the resulting mixture was transferred to stainless steel autoclave and loaded into an oven preheated to 160 °C for 1 hr. Subsequently, the reaction system was cooled to 50°C, the suspension was filtered with a Millopore filter (pore diameter, 0.45μm) and the as-obtained product was washed with DI water and absolute ethanol. Finally, the black precipitates were collected and annealed at 300°C in nitrogen for 3hr.

### *2.2. Preparation of the composite modified glass carbon electrode*

The electrochemical experiments were carried out on a CHI 660E electrochemical workstation (CH Instrument, Shanghai) using a three-electrode system at room temperature. A saturated calomel

electrode (SCE) and Pt plate were used as the reference and counter electrode, respectively. The working electrode was prepared by mixing the $MnO_2$@MWNT composite with poly(tetrafluoroethylene) (PTFE) and carbon black (CB), and the weight ratio of composite: PTFE: CB = 80:10:10. During the making working electrode step, 10 mg mixture was pressing on Ni foam (1 ×1.5cm$^2$), which was dried at 80◦C in a vacuum oven for 3 h. The cyclic voltammetry (CV) and galvanostatic charging/discharging techniques were employed to investigate the electrochemical performance of the working electrode. The *C*s is calculated according to $Cs = I \times \Delta t/(\Delta V \times m)$ from the discharge curves, where $I$ is the constant discharge current, $\Delta t$ is the discharge time, and $\Delta V$ is the potential drop during discharge.

### *2.3. Characterization*

TEM images were achieved on a JEOL JEM-2010 transmission electron microscope operated at an accelerating voltage of 200 kV. The samples were prepared by drying a droplet of the composite suspensions on a Cu grid. The structure of the samples was examined by XRD, Shimadzu, X-6000, Cu Kα radiation (λ= 0.154 nm)). XPS analyses were carried out using a Thermo Fisher X-ray photoelectron spectrometer equipped with Al radiation as the probe. Thermogravimetric analysis (TGA) data were collected on a thermal analysis instrument (NETZSCH STA 449C) with heating rate of 10 °C/min in an air.

## 3. RESULT AND DISCUSSION

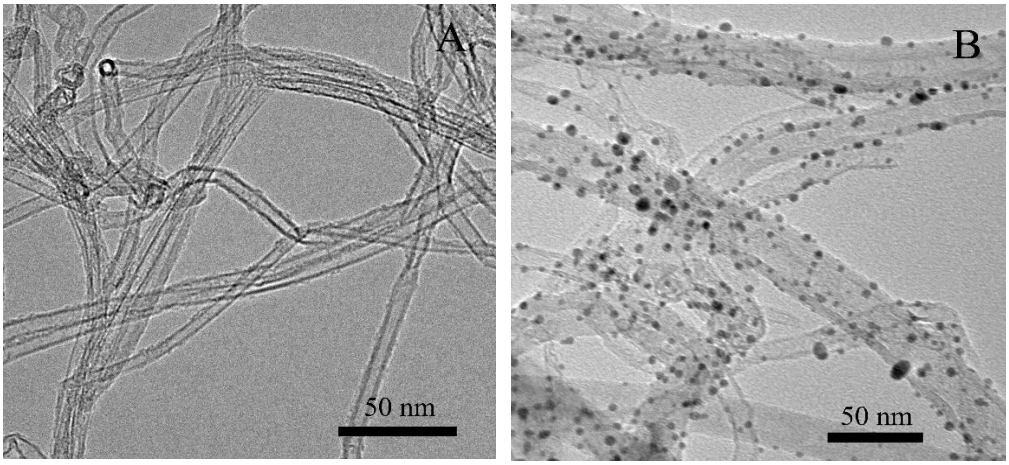


**Figure 1**. TEM images of MWNT and $MnO_2$@MWNT nanocomposite.

The morphology of MWNT and $MnO_2$@MWNT nanocomposite was investigated by TEM. Figure 1A shows the clean carbon nanotubes with a perfect tube morphology. A majority of MWNTs exhibit uniform diameter about 10 nm. In general, MWNTs possess large specific surface area, which makes the tubes adjust themselves physically to adapt the different types of electrolytes. Figure 1B is the typical TEM image of as-obtained $MnO_2$@MWNT nanocomposite. Highly dispersed $MnO_2$

nanoparticles uniformly distributed on the surface of MWNTs can provide large available surface and enhance the electrocatalytic activity. PVP used here is the reducing and stabilizing reagent for preparation the $MnO_2$@MWNT composites. Such protuberant structure enables more electrochemically active surface area of $MnO_2$ to be accessed by the electrolyte, promoting the surface redox reaction and EDLC formation.

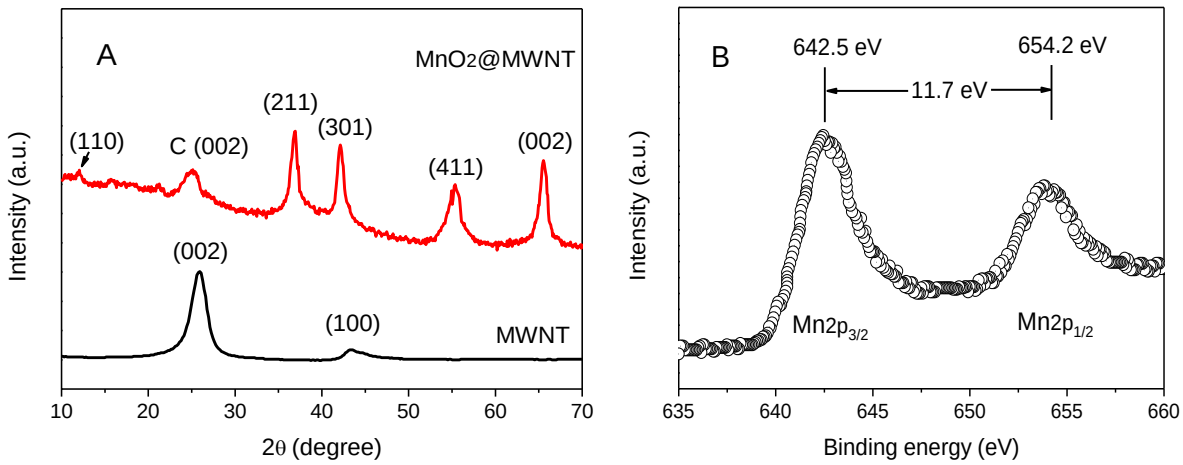


**Figure 2**. (A) XRD patterns of the MWNTs and $MnO_2$@MWNTs, (B) High-resolution XPS spectra of Mn2p.

The XRD spectra of the $MnO_2$@MWNT composite are shown in Figure 2 A. A strong diffraction peak at $2\theta = 25.8°$ is due to the (002) diffraction of graphite from the MWNT, while the peaks at $2\theta = 11.8°$, 36.8°, 41.6°, 55.2° and 65.3° can be indexed to the (110), (211), (301), (411) and (002) reflections of α-$MnO_2$ (JCPDS 44-0141), respectively[17, 18]. It confirms that the manganese precursor $MnCl_2$ had been oxidated to $MnO_2$ by $H_2O_2$.

Figure 2B presents high-resolution XPS spectra of Mn2p. The two peaks are centered at binding energies (BEs) of 642.5 and 654.2 eV, respectively. A spin-energy separation of 11.7 eV was observed between the two peaks, which is in good agreement with the published data for Mn $2p_{3/2}$ and Mn $2p_{1/2}$ in $MnO_2$ [19]. This result is also consistent with the results of X-ray diffraction analysis.

Figure 3 depicts the weight-loss curves by heating the $MnO_2$@MWNT samples in air at a heating rate of 10 ℃/min. Below 200 ℃, a gradual decrease in composite mass is found because of the removal of adsorbed moistures and intercalated water. The sharp mass loss about 450 ℃ is attributed to the consumption of MWNTs. Above 700 ℃, No apparent weight loss is observed. MWNTs are completely consumed, while $MnO_2$ is transformed to thermodynamically stable $Mn_2O_3$ [20]. According to the residual mass of $Mn_2O_3$, the $MnO_2$ contents in the synthesized $MnO_2$@MWNT composites were calculated to be 34.43%.

The capacitive behavior of MWNT and $MnO_2$@MWNT electrodes was investigated by CV and galvanostatic charge−discharge (GCD) in a three-electrode system with 1.0 mol/L $Na_2SO_4$ electrolyte. The potential window of CV measurements was chosen from 0 to 0.8 V versus SCE with a scan rate of

10 mV/s. The CV curve for the MWNTs@GCE exhibits a rectangular shape corresponding to ideal EDLC with a very rapid current response at a scan rate of 10 mV $s^{-1}$ as shown in Figure.

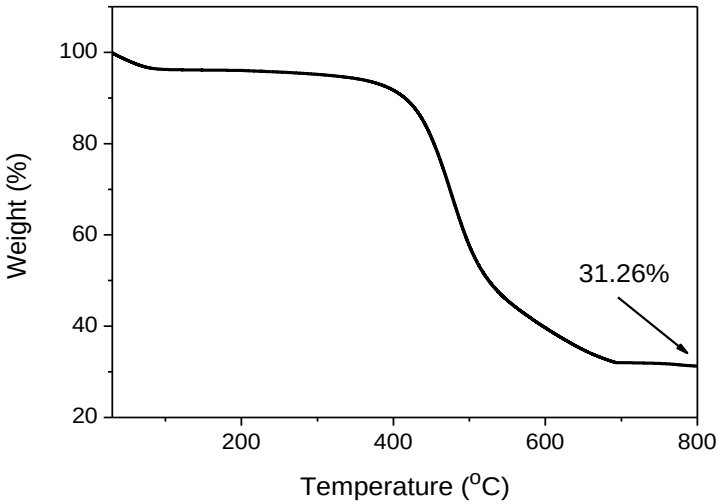


**Figure 3**. TGA curves of the $MnO_2$@MWNT composite.

4A. Moreover, the *CV* curves for $MnO_2$@MWNT shows near-rectangular shapes without evident redox peaks, indicating the fact that Faraday redox reactions are electrochemically reversible [21].

The charge storage mechanisms of $MnO_2$ were put forward in mild $Na_2SO_4$ aqueous electrolyte, involving surface adsorption/desorption of $Na^+$, which were expressed as equation [22].

(O=Mn=O) surface + $Na^+$ + e → (O=Mn=O $Na^+$) surface

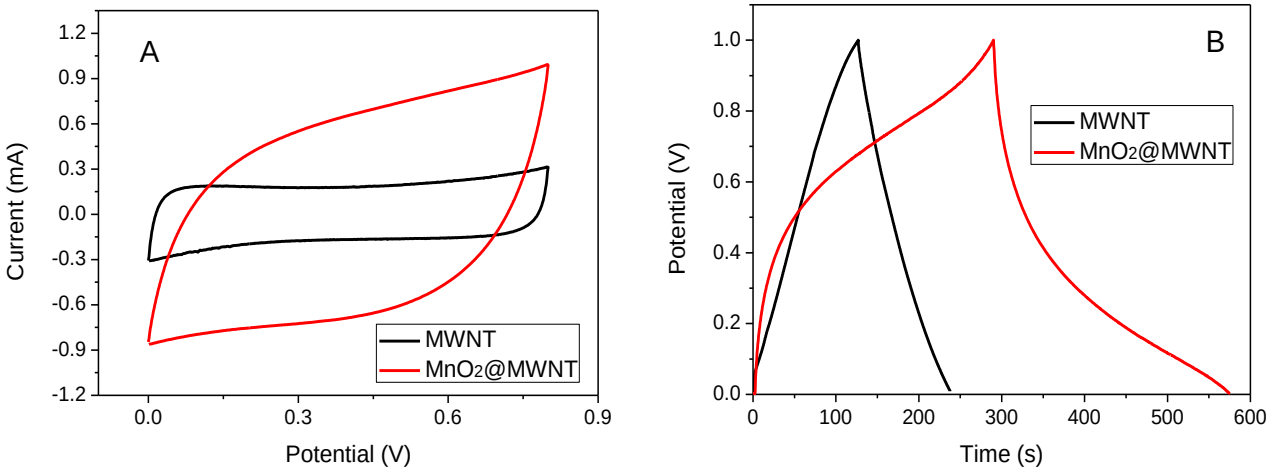


**Figure 4**. (A) CV curve of MWNTs and $MnO_2$@MWNT with a scan rate of 10mV $s^{-1}$, (B) Galvanostatic charge/discharge curves of MWNTs and $MnO_2$@MWNT at 1A/g.

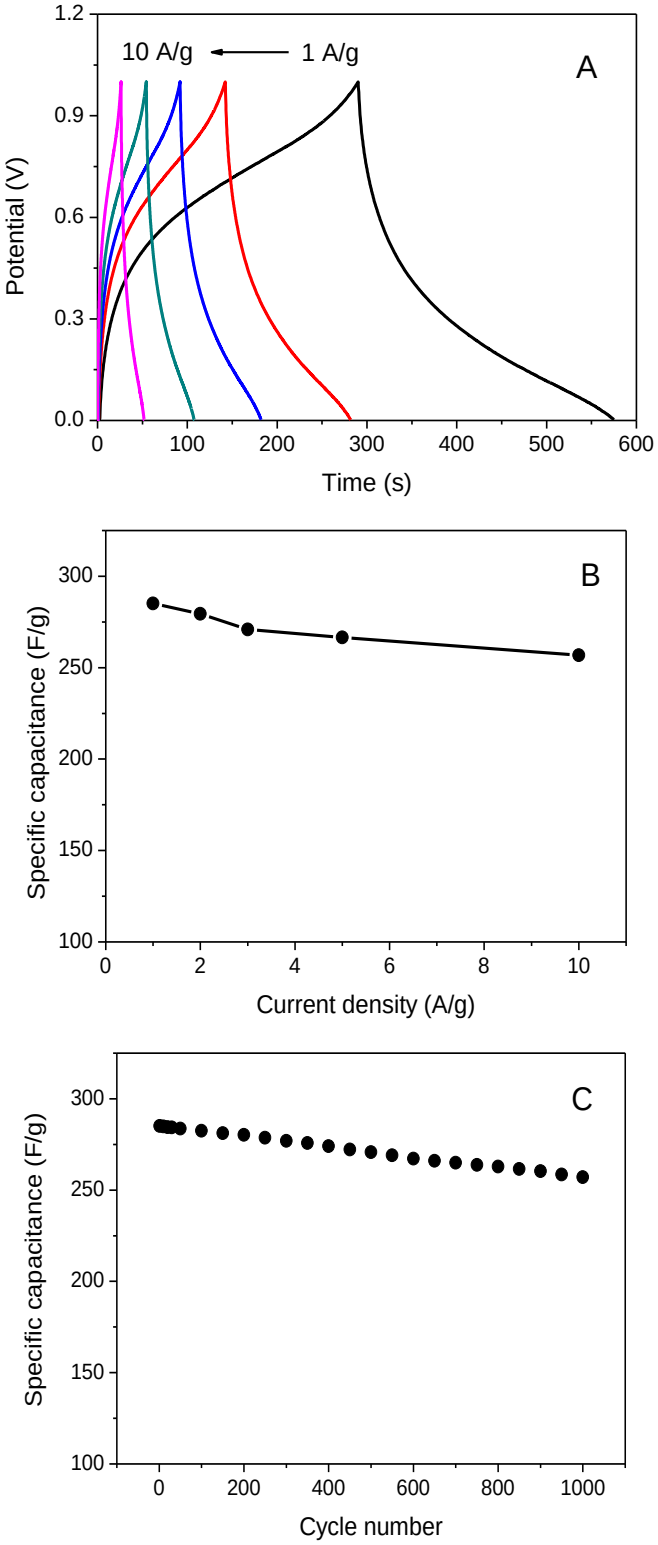


**Figure 5**. (A) GCD curves at different current densities ranging from 1 A/g to 10 A/g , (B) Variation of the specific capacitance with current density for $MnO_2$@MWNT, (C) Cycle performance of $MnO_2$@MWNT at 1 A/g.

The GCD curves of MWNTs and $MnO_2$@MWNT electrodes in 1 M $Na_2SO_4$ solution were carried out at 1 A/g. The MWNTs and $MnO_2$@MWNT exhibit nearly symmetric charge-discharge curve which implies its good electrochemical reversibility as shown in Figure 4B. The specific

capacitance of $MnO_2$@MWNT (285.12 F/g) is much higher than that of MWNT (110.80 F/g) at the same current density. The result shows $MnO_2$ played a critical role in enhancing the specific capacitance.

In order to further estimate the capacitive behavior of $MnO_2$@MWNT hybrids, GCD measurements were applied at various current densities. Figure 5A shows the GCD of $MnO_2$@MWNT electrode at current densities from 1 to 10 A/g between 0 and 1 V (vs. SCE). The near symmetrical charge and discharge profiles can be obtained, which indicates typical and excellent capacitive property of the composites. It is consistent with CV observations.

The specific capacitance derived from the discharge curve is calculated to be 285.12 F/g at a current density of 1A/g; while at 10 A/g, the $MnO_2$@MWNT electrode still has a discharge capacitance of 256.76 F/g. The corresponding rate performance is clearly observed from Figure 5B. At 10 A/g, the $MnO_2$@MWNT electrode still possesses 90.05% of its specific capacitance at 1A/g. The high electrochemical capacitive characteristics is attributed to the introduction of well-dispersed and nanoscale $MnO_2$ on the conductive MWNT surfaces.

The cycle stability of supercapacitor is a key parameter in the practical applications. A lot of documents show excellent cycling stability of EDLCs consisting of carbon nanomaterials owing to the nonexistence of pseudocapacitance effect. [23, 24] As for pseudocapacitive materials of conducting polymers, metal oxides and others, the cycle life is much shorter than carbon-based materials because of changes of structure or volume during redox reactions leads to the loss of active materials. [25, 26] The cycling stability of $MnO_2$@MWNT was measured by GCD test in 1 M $Na_2SO_4$ shown in Figure 5C. In the first cycle, the capacitance is about 285.12 F/g with a coulombic efficiency of nearly 100%. After 1000 cycles, the capacitance slightly decreases to around 257.08 F/g, indicating an excellent capacitance retention as high as 90.17%. In virtue of these features, the $MnO_2$@MWNT composites may be a promising material for high-performance supercapacitors.

## 4. CONCLUSION

$MnO_2$@MWNT composite has been synthesized via PVP-assisted reaction through facile hydrothermal process. The as-prepared composite exhibits an excellent electrochemical performance as supercapacitor, because of the electrochemical activities of embedded $MnO_2$ nanoparticles attached to the surface of MWNTs. A high specific capacitance of 285.12 F/g has been achieved for $MnO_2$@MWNT composite, which is almost doubled over that of pure MWNTs. The specific capacitance retention retains up to 90.17% after 1000 cycles at 1 A/g. Based on low cost, environmental friendly nature and excellent capacitive properties, the $MnO_2$@MWNT composite is a promising pseudocapacitive electrode material for supercapacitors.

ACKNOWLEDGEMENTS
This work was supported by the National Natural Science Foundation of China (21565002, 21505016), Program for Changjiang Scholars and Innovative Research Team in University (IRT13054), Young Scientist Foundation of Jiangxi Province (20133BCB23020) and Most Foundation of Jiangxi Province (20152ACB21018).

**References**


1. H.L. Li, L.X. Jiang, Q.L. Cheng, Y. He, V. Pavlinek, P. Saha, C.Z. Li, *Electrochimica Acta*. 164 (2015) 252.
2. P. Simon, Y. Gogotsi, *Nat. Mater*. 7 (2008) 845.
3. D. Zhou, H.M. Lin, F. Zhang, H. Niu, L.R. Cui, Q. Wang, F.G. Qu, *Electrochimica Acta*. 161 (2015) 427.
4. S.B. Yoon, K.B. Kim, *Electrochimica Acta*. 106 (2013) 135.
5. X. Zhao, B.M. Sanchez, P.J. Dobson, P.S. Grant, *Nanoscale*. 3 (2011) 839.
6. C.Y. Xiong, T.H. Li, A.L Dang, T.K. Zhao, H. Li, H.Q. Lv, *Journal of Power Sources*. 306 (2016) 602.
7. S. Iijima, *Nature*. 354 (1991) 56.
8. K. Koziol, J. Vilatela, A. Moisala, M. Motta, P. Cunniff, M. Sennett, A. Windle, *Science*. 318 (2007) 1892.
9. C. Luo, R.Y. Wei, D. Guo, S.F. Zhang, S.Q. Yan, *Chemical Engineering Journal*. 225 (2013) 406.
10. Y. Zhai, Y. Dou, D. Zhao, *Adv. Mater.* 23 (2011) 4828.
11. A.C. Dillon, *Chem. Rev*. 110 (2010) 6856.
12. L.L. Zhang, X.S. Zhao, *Chem. Soc. Rev.* 38 (2009) 2520.
13. Q. Mahmood, H.J. Yun, W.S. Kim, H.S. Park, *Journal of Power Sources*. 235 (2013) 187.
14. M. Li, F. Liu, J.P. Cheng, J. Ying, X.B. Zhang, *J. Alloy. Compd*. 635 (2015) 225.
15. M. Li, K.Y. Ma, J.P. Cheng, D.H. Lv, X.B. Zhang, *Journal of Power Sources*. 286 (2015) 438.
16. Y.C. Li, S.Q. Feng, S.X. Li, Y.Y. Zhang, Y.M. Zhong, *Sens. Actuators B*. 190 (2014) 999.
17. D.W. Xu, B.H. Li, C.G. Wei, Y.B. He, H.D. Du, X.D. Chu, X.Y. Qin, Q.H. Yang, F.Y. Kang, *Electrochimica Acta*. 133 (2014) 254.
18. D.K. Walanda, G.A. Lawrance, S.W. Donne, *J. Power Sources.* 139 (2005) 325.
19. X. Dong, W. Shen, J. Gu, L. Xiong, Y. Zhu, H. Li, J. Shi, *J. Phys. Chem. B*. 110 (2006) 6015.
20. X.L. Wang, X.Y. Fan, G. Li, M. Li, X.C. Xiao, A.P. Yu, Z.W. Chen, *Carbon*. 93 (2015) 258.
21. T. Xue, C. Xua, D. Zhao, X. Li, H. Li, *J. Power Sources.* 164 (2007) 953.
22. W. Wei, X. Cui, W. Chen, D.G. Ivey, *Chem. Soc. Rev*. 40 (2011) 1697.
23. P. Simon, Y. Gogotsi, *Nat. Mater.* 7(2008)845.
24. H. Jung, W. Lee, W. Shin, Y. J. Choi, H.J. Shin, J.K. Kang, *Nano Lett.* 11(2011) 2472.
25. T. Fukushima, A. Kosaka, Y. Yamamoto, T. Aimiya, S. Notazawa, T. Takigawa, *Small*. 2(2006) 554.
26. E. Frackowiak, F. Beguin, *Carbon*. 39 (2016) 937.